ELSEVIER

Hearing Research 148 (2000) 107–123

HEARING RESEARCH

www.elsevier.com/locate/heares

Latency as a function of intensity in auditory neurons: influences of central processing

Achim Klug [a,b], Asma Khan [a], R. Michael Burger [b], Eric E. Bauer [b], Laura M. Hurley [b], Lichuan Yang [b], Benedikt Grothe [c], Michele B. Halvorsen [a], Thomas J. Park [a,*]

[a] *The Neurobiology Group, Department of Biological Sciences, University of Illinois at Chicago, 845 W. Taylor Street, M/C 066, Chicago, IL 60607, USA*

[b] *Section of Neurobiology, University of Texas, Austin, TX 78712, USA*

[c] *Max Planck Institut für Neurobiologie, Martinsried, Germany*

Received 5 May 2000; accepted 6 June 2000

Abstract

The response latencies of sensory neurons typically shorten with increases in stimulus intensity. In the central auditory system this phenomenon should have a significant impact on a number of auditory functions that depend critically on an integration of precisely timed neural inputs. Evidence from previous studies suggests that the auditory system not only copes with the potential problems associated with intensity-dependent latency change, but that it also modifies latency change to shape the response properties of many cells for specific functions. This observation suggests that intensity-dependent latency change may undergo functional transformations along the auditory neuraxis. The goal of our study was to explore these transformations by making a direct, quantitative comparison of intensity-dependent latency change among a number of auditory centers from the lower brainstem to the thalamus. We found two main ways in which intensity-dependent latency change transformed along the neuraxis: (1) the range of latency change increased substantially and (2) one particular type of latency change, which has been suggested to be associated with sensitivity to temporally segregated stimulus components, occurred only at the highest centers tested, the midbrain and thalamus. Additional testing in the midbrain (inferior colliculus) indicated that inhibitory inputs are involved in shaping latency change. Our findings demonstrate that the central auditory system modifies intensity-dependent latency changes. We suggest that these changes may be functionally incorporated, actively enhanced, or modified to suit specific functions of the auditory system.

Key words: Latency; Auditory neurons; Central processing; Central auditory system

1. Introduction

The response latency of sensory neurons typically shortens with increases in stimulus intensity, a phenomenon commonly known as 'intensity-dependent latency change'. This type of latency change has been demonstrated in a number of sensory systems, including the visual (e.g. Carney et al., 1989; Kolehmainen and Keskinen, 1974; Lit, 1949; Pulfrich, 1922), somatosensory (e.g. Mountcastle et al., 1957), and auditory system (e.g. Aitkin et al., 1970; Brugge et al., 1969; Deatherage et al., 1959; Goldberg and Brownell, 1973; Hind et al., 1963; Kitzes et al., 1978). Because many auditory functions depend critically on a precise timing of neural inputs (reviewed by Covey and Casseday, 1999; Oertel, 1999), one would expect that intensity-dependent latency change would have an especially significant impact on auditory processing.

In the auditory system, intensity-dependent latency change has been observed at many auditory stations, including the cochlea (guinea pig, Deatherage et al., 1959), cochlear nucleus (cat, Goldberg and Brownell, 1973; Kitzes et al., 1978; rat, Møller, 1975), superior olivary complex (gerbil, Sanes and Rubel, 1988), lateral lemniscus (cat, Aitkin et al., 1970; bat, Haplea et al., 1994), inferior colliculus (cat, Hind et al., 1963; Irvine

* Corresponding author. Tel.: +1 (312) 413-3020; Fax: +1 (312) 413-2435; E-mail: tpark@uic.edu

0378-5955/00/$ – see front matter
PII: S0378-5955(00)00146-5

and Gago, 1990; bat, Bodenhamer and Pollak, 1981; Haplea et al., 1994), medial geniculate body (cat, Aitkin and Dunlop, 1968), and auditory cortex (cat, Brugge et al., 1969). The mechanisms underlying intensity-dependent latency change in sensory systems are not fully known, and there is evidence for both peripheral and central effects.

In support of peripheral mechanisms, Eccles (1964) suggested that intensity-dependent latency change may be largely due to factors such as temporal summation at receptor cells, or the summing of excitatory postsynaptic potentials at neurons receiving synaptic inputs from receptor cells. In the auditory system, studies by Heil (1997a,b, 1998) and Heil and Irvine (1996, 1997, 1998) support a peripheral mechanism in establishing intensity-dependent latency change. Those authors recorded first spike latencies from auditory nerve fibers and from neurons in primary auditory cortex, and their data resulted in two important findings.

The first finding was that the same average intensity-dependent latency shift was observed at the auditory nerve and auditory cortex, thus suggesting that the effect is established at the periphery (Heil and Irvine, 1997). The second important finding was that the term '*intensity*-dependent latency change' is to some extent a misnomer. For tone stimuli, the word 'intensity' usually refers to the peak amplitude of the steady-state portion of the tone. However, the work by Heil and Irvine showed that first spike latency is more dependent on the characteristics of a tone's transient onset portion than on the steady-state portion of the tone. Because tone bursts are designed with specific rise times, and these rise times are kept constant throughout different intensities, the onset characteristics of a tone co-vary with peak sound pressure level. Specifically, these studies show that first spike latency depended more on the maximum acceleration of peak pressure during the rise time than on the steady-state peak pressure per se (Heil, 1997a; Heil and Irvine, 1997).

On the other hand, there is also evidence that, within the central auditory system, intensity-dependent latency change undergoes substantial modification, presumably due to central processing. The evidence comes from studies that indicate differences in intensity-dependent latency change from nucleus to nucleus, and from one synaptic level to another. For example, auditory nerve fibers are characterized by a moderate decrease in latency with increasing intensities of the order of 25 μs/dB for intensities greater than 10 dB above threshold (Heil and Irvine, 1997; Antoli-Candela and Kiang, 1978). In contrast, cells that show a much smaller latency change with intensity, termed constant latency cells, have been observed in a variety of higher auditory nuclei (Batra and Fitzpatrick, 1999; Bodenhamer and Pollak, 1981; Covey, 1993; Covey and Casseday, 1991; Suga, 1970), and comprise the dominant response type in one auditory brainstem region, the columnar area of the ventral nucleus of the lateral lemniscus (Covey and Casseday, 1991).

A second variation concerns neurons termed paradoxical latency cells that show an *increase* in latency with intensity. Paradoxical latency cells appear to be much more prevalent in the midbrain and above compared to regions below the midbrain (Berkowitz and Suga, 1989; Olsen and Suga, 1991a,b; Rose et al., 1959; Suga, 1970; Sullivan, 1982; Aitkin et al., 1970; Covey, 1993). If intensity-dependent latency change were determined only by peripheral phenomena, then one would not expect to see these types of regional differences at higher synaptic levels.

In order to better assess the potential role of central processing in shaping intensity-dependent latency shifts, we measured these shifts in five nuclei along the ascending auditory system of Mexican free-tailed bats. To determine if our results are species-specific or general, we repeated some of the analyses in two other species, the mustache bat and the Mongolian gerbil. For each nucleus we used identical experimental procedures, stimulation protocols and data analyses. By comparing results between different nuclei we were able to observe several features of intensity-dependent latency shifts that could be attributed to central processing.

2. Methods

The goal of the present report was to more directly assess the role of central processing in shaping intensity-dependent latency change by performing a quantitative analysis among a variety of auditory nuclei within a single species, using a single rise time. To do so, we re-analyzed data that we had collected over the past 7 years, focusing on intensity-dependent latency change. Most of the data that we used were originally collected to address other questions about auditory processing. The cells we studied were recorded from 38 Mexican free-tailed bats (*Tadarida brasiliensis mexicana*), 69 mustache bats (*Pteronotus parnellii*), and 14 Mongolian gerbils (*Meriones unguiculatus*). Some of the cells used for the present analysis were initially recorded for previous studies that focused on other aspects of auditory processing (Bauer et al., 2000; Burger and Pollak, 1998; Grothe, 1994; Grothe and Park, 1998; Klug et al., 1999; Park et al., 1996, 1997; Yang and Pollak, 1994a,b).

2.1. Surgical procedures for bats

Bats were anesthetized with methoxyflurane inhalation (Metofane, Schering-Plough Animal Health) and

either 10 mg/kg sodium pentobarbital (Abbott Laboratories), or 10 mg/kg Vetamine (Innovar-Vet, Schering-Plough) injected subcutaneously. The bat's head was secured in a head holder with a bite bar, and the hair was removed from the top of the head with a depilatory. The muscles and skin overlying the skull were reflected, and 2% or 4% lidocaine hydrochloride (Abbott Laboratories) was applied topically to the open wound. The wound edges of the scalp were then treated with a commercially available triple antibiotic cream (bacitracin zinc, neomycin, and polymyxin b sulfate), and secured to the skull with Vet Bond (3M Animal Care), leaving the top portion of the skull exposed while protecting the incision from exposure to air. The exposed surface of the skull was cleared of tissue and a ground electrode was placed under the scalp or just beneath the skull over the posterior cerebellum. A layer of small glass beads and dental acrylic was placed on the surface of the skull to serve as a foundation layer to be used later for securing a metal rod to the head.

The bat was then transferred to a heated (27–30°C), sound-attenuated room, where it was placed in a restraining apparatus attached to a custom-made stereotaxic instrument (Schuller et al., 1986). A small metal rod was cemented to the foundation layer on the skull and then attached to a bar mounted on the stereotaxic instrument to ensure uniform positioning of the head. A small hole (approximately 0.5–1.0 mm in diameter) was cut in the skull to allow electrode access. Position of the hole and positioning of the electrode to reach target nuclei generally followed procedures described by Schuller et al. (1986). Recordings were begun after the bat was awake. On several occasions, an additional subanesthetic injection of sodium pentobarbital (5 mg/kg), or Innovar-Vet (0.005 ml/g) was given subcutaneously. This dosage did not induce anesthesia: the bats were still awake in that their eyes were open, they often drank water when it was offered, and they responded when their face or ears were gently touched. There were no noticeable, systematic changes in neuronal response properties from the subanesthetic dose. Additional injections were administered on only a few occasions and then only once during a given recording session. Recording sessions generally lasted 3–5 h per day to minimize the animals' discomfort from being restrained. On average, bats were tested on 5 consecutive days (sessions). Between sessions, experimental animals were housed separately, the surgical incision site was monitored twice daily for signs of infection, and overall behavior (e.g. food and water intake, movement within the home cage, and responsiveness to touch) was monitored for signs that the animal was in discomfort.

2.2. Surgical procedures for gerbils

Procedures for gerbils were the same as those for bats with the following exceptions. Gerbils were maintained under anesthesia throughout an experiment with a mixture of ketamine (100 mg/kg) and xylazine (5 mg/kg) (Ben Venue Laboratories). A heating pad with rectal probe was used to maintain body temperature at 33°C. To access the inferior colliculus, a hole was cut over the cerebellum and a small portion of cerebellum was suctioned away. Gerbils were used for one recording session only and killed immediately after the session.

2.3. Identification of recording sites

For all nuclei except the inferior colliculus, the locations of recording sites were confirmed by small iontophoretic injections of horseradish peroxidase (HRP, Sigma Chemicals) or rhodamine-conjugated dextran (Molecular Probes) made after all recordings were completed in each animal (one injection per animal). Twenty-four hours after the injection, the animal was deeply anesthetized and perfused through the heart with buffered saline and a mixture of 4% paraformaldehyde and 1% glutaraldehyde (HRP) or 4% paraformaldehyde (dextran). The brain was dissected out, frozen, and cut into 40 μm sections, which were then processed for HRP reaction product. In each case the HRP deposit was located within the target nucleus. Since we usually used different, stereotaxically placed electrodes for HRP and for recording, HRP deposit sites did not correspond precisely to recording sites. However, given that limitation, it was reassuring that the HRP sites were consistent with our stereotaxic placements.

The inferior colliculi of both bat species and the gerbil are easily identified by visual landmarks and thus, tracer injections were not used. For the gerbils, we only recorded from the inferior colliculus and hence, tracers were never used with the gerbils.

Within the inferior colliculus, we targeted the central division (= ICc) using visual landmarks to place electrodes. For the bats, we penetrated through the external division of the inferior colliculus, located just beneath the skull, by driving the electrode to a depth of greater than 300 μm before taking data. Similarly, for the gerbils, we visually placed the electrode on the exposed surface of the IC, and then drove the electrode to sufficient depth to pass the peri-central nucleus.

2.4. Acoustic stimuli and data acquisition

Action potentials were recorded with a glass pipette filled with buffered 1 M NaCl or 1 M KCl, and elec-

trode impedance ranged from 5 to 20 MΩ. The electrode was advanced from outside the experimental chamber with a piezoelectric microdrive. When a neuron was encountered, we first determined its characteristic frequency and absolute threshold audio-visually in order to set stimulus parameters subsequently controlled by computer. The characteristic frequency (CF) was defined as the frequency that elicited responses at the lowest sound intensity to which the unit was sensitive.

Each cell was tested with 20 or 60 ms tones presented at a rate of 4/s. Tone stimuli were presented at a cell's CF with 0.2 ms rise and fall times shaped by a sigmoid. Stimuli were presented via Brüel and Kjaer 1/4 inch microphones used as ear phones (bats), or Gemini Industries Model AS4 earphones fitted with probe tubes of 5 mm diameter (gerbils) that were placed in the funnel of each pinna. Sound pressure and the frequency response of each earphone was calibrated with a 1/4 inch Brüel and Kjaer microphone. Each earphone showed less than ±8 dB variability over the frequency range usually used (18–80 kHz for bats, 2–40 kHz for gerbils). For fundamentals of less than 50 kHz, all harmonics were at least 35 dB less intense than the fundamental. For higher frequencies the harmonics were even lower. Acoustic isolation between the ears was better than 40 dB (e.g. Oswald et al., 1999).

Rate–intensity functions were generated for each cell by varying the stimulus intensity in 5 or 10 dB steps. Each stimulus intensity was presented 20 times, and the order in which different intensities were presented was varied pseudo-randomly. To determine the intensity-dependent latency change for an individual cell, we first determined its response latency for each intensity from the rate level function. The latency of the first spike to each stimulus presentation at a given intensity was used to calculate the median value of first spike latency for that intensity. Presumably, by taking the median value (as opposed to the mean), we minimized the effects of any errant spontaneous spikes, as well as spikes that occurred with an unusually long latency. For intensities near threshold, many cells responded with less than one spike per stimulus, and hence, median values were based only on trials that evoked a spike. Only spikes occurring within 100 ms of stimulus onset were included in the calculation of the median first spike value. Median first spike latency values for each intensity tested were then used to calculate changes in latency as a function of intensity.

Data from each nucleus were generated by stimulating the ear associated with the more prominent excitation in that nucleus. Hence, for cells in the lateral superior olive (LSO), we stimulated the ipsilateral ear, and in each of the other nuclei, we stimulated the contralateral ear (e.g. Bauer et al., 2000; Burger and Pollak, 1998; Grothe, 1994; Grothe and Park, 1998; Klug et al., 1999; Park et al., 1996, 1997; Yang and Pollak, 1994a,b).

The intensities we used to generate rate–intensity functions always ranged 10–30 dB above a cell's threshold, and usually they ranged up to 50 dB above threshold. We limited the highest intensity to 50 dB above threshold because, with our earphone system and the frequencies we usually employed, we could not maintain acoustic isolation between the ears for intensities greater than 50 dB above a cell's threshold. Hence, limiting our highest intensity ensured that our data were consistently from monaural stimulation, an important consideration since many of our cells were binaural. The main reason some cells were tested with an even more limited range of intensities is because either we failed to record data at these intensities, or the cells were nonmonotonic and failed to respond at these intensities.

Twenty-four cells in the free-tailed bat ICc and 39 cells in the mustache bat ICc were tested before and during micro-iontophoretic application of the γ-aminobutyric acid A ($GABA_A$) antagonist, bicuculline, following established procedures (Havey and Caspary, 1980; Park and Pollak, 1993b).

2.5. Experimental procedures

The experimental protocols were approved by the

Table 1
Nuclei tested, number of cells tested in each nucleus, and range of characteristic frequencies of cells encountered within each nucleus

	MSO	LSO	DNLL	ICc	MGv
Tadarida	$n = 19$ 9.0–81.0 kHz $\bar{x} = 36.0$ kHz	$n = 58$ 14.4–57.5 kHz $\bar{x} = 32.6$ kHz	$n = 89$ 17.4–86.7 kHz $\bar{x} = 38.1$ kHz	$n = 164$ 17.6–54.0 kHz $\bar{x} = 27.3$ kHz	$n = 101$ 11.8–86.3 kHz $\bar{x} = 45.1$ kHz
Pteronotus	$n = 32$ 16.9–113.0 kHz $\bar{x} = 69.0$ kHz	$n = 117$ 19.0–113.7 kHz $\bar{x} = 67.4$ kHz	$n = 143$ 17.3–113.5 kHz $\bar{x} = 68.4$ kHz	$n = 157$ 33.8–63.9 kHz $\bar{x} = 60.6$ kHz	
Meriones				$n = 68$ 2.0–40.0 kHz $\bar{x} = 14.0$ kHz	

University of Illinois at Chicago Institutional Animal Care and Use Committee, and the University of Texas Institutional Animal Care and Use Committee.

3. Results

The goal of this study was to compare intensity-dependent latency change among nuclei at several synaptic levels in the central auditory system. The nuclei we studied were the medial superior olive (MSO), the LSO, the dorsal nucleus of the lateral lemniscus (DNLL), the ICc, and the ventral nucleus of the medial geniculate (MGv). In this report, we first present data from the Mexican free-tailed bat, we then present comparative data from the mustache bat and the Mongolian gerbil. Table 1 lists the numbers of cells included in the analysis of each nucleus, and the range of characteristic frequencies for each sample population.

To make comparisons of intensity-dependent latency change among nuclei, we first measured the response latency of each cell at different stimulus intensities, usually 10–50 dB above a cell's threshold. We then calculated the latency change associated with each incremental increase in intensity. To show how these measures were made, dot rasters from an LSO cell and an IC cell

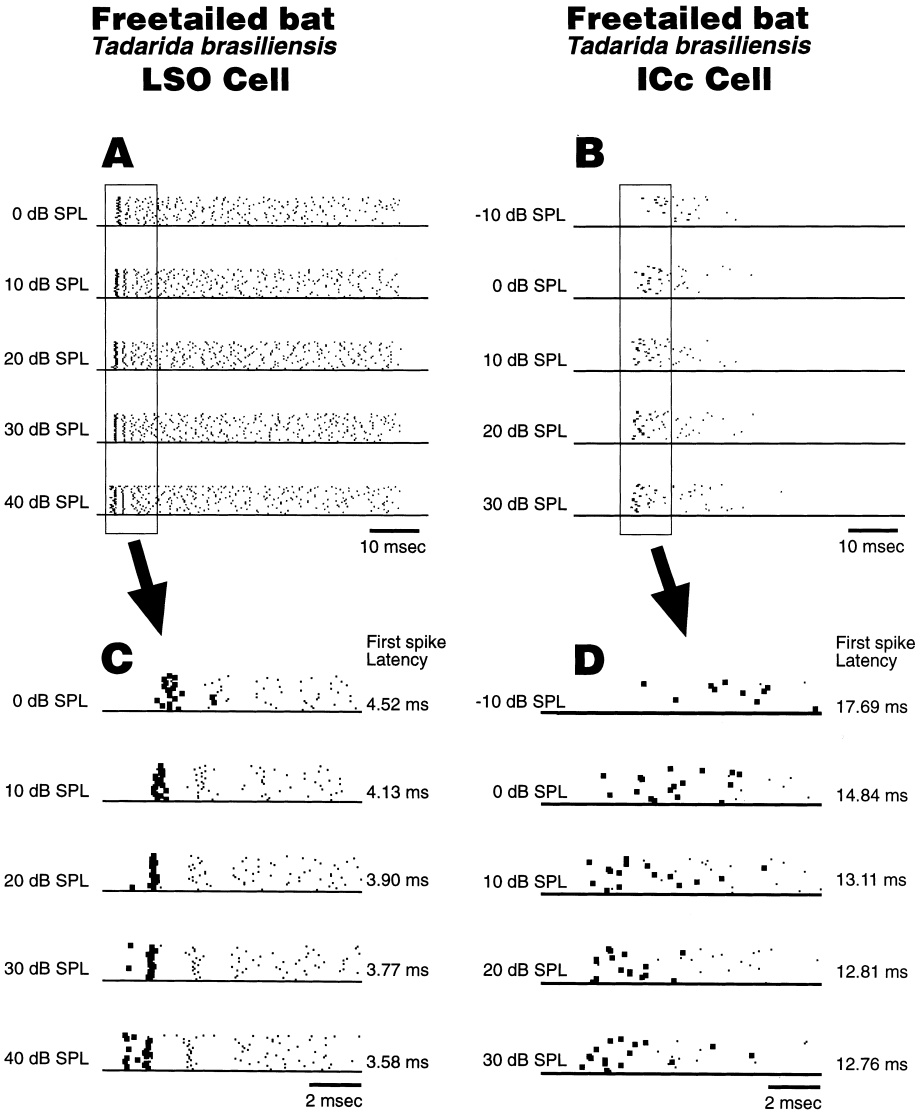

Fig. 1. Dot raster plots from an LSO cell (A and C), and an ICc cell (B and D), illustrating spike activity to five suprathreshold stimulus intensities. Each intensity was presented 20 times, and the first spike in response to each stimulus presentation is shown in bold. In A and B, the window shown for each plot is 70 ms from stimulus onset. To help visualize latency change as a function of intensity, the initial spike activity from A and B is replotted in C and D on a 10 ms, expanded time scale beginning 2 ms after stimulus onset in C and 10 ms after stimulus onset in D. Median first spike latencies are indicated to the right of each plot. Stimuli were 60 ms tones, presented at the frequency to which each cell was most sensitive (a cell's CF). CF of the LSO cell was 31.3 kHz; CF of the ICc cell was 25.8 kHz.

are presented in Fig. 1 at two different time scales. The first spike in response to each stimulus repetition is highlighted in bold, and the median latency value of first spikes at each intensity is indicated on the right. For the LSO cell, the median first spike latency shortened from 4.52 ms at 0 dB SPL to 3.58 ms at 40 dB SPL. Hence, this cell showed an average latency change of 24 μs/dB over the range of intensities tested. Because we limited the maximum intensity to 50 dB above a cell's threshold, the data we collected did not necessarily reflect a cell's full dynamic range.

Latency data for the ICc neuron are shown in Fig. 1B,D. The absolute latency of responses was much longer for the ICc cell compared to the LSO cell. However, a more important observation for the present study was that the average latency change with intensity was very different for the ICc cell and the LSO cell. For the ICc cell, the median first spike latency shortened from 17.69 ms at −10 dB SPL to 12.76 ms at 30 dB SPL, an average latency change of 123 μs/dB, a five-fold increase compared to the LSO cell. In the sections below we will address this key issue by presenting both population data and data from individual cells.

In the following sections we will first present the mean latencies and ranges of latencies that we observed for each nucleus, and how those population values changed with intensity. Then we will focus on the patterns and magnitudes of latency change observed for

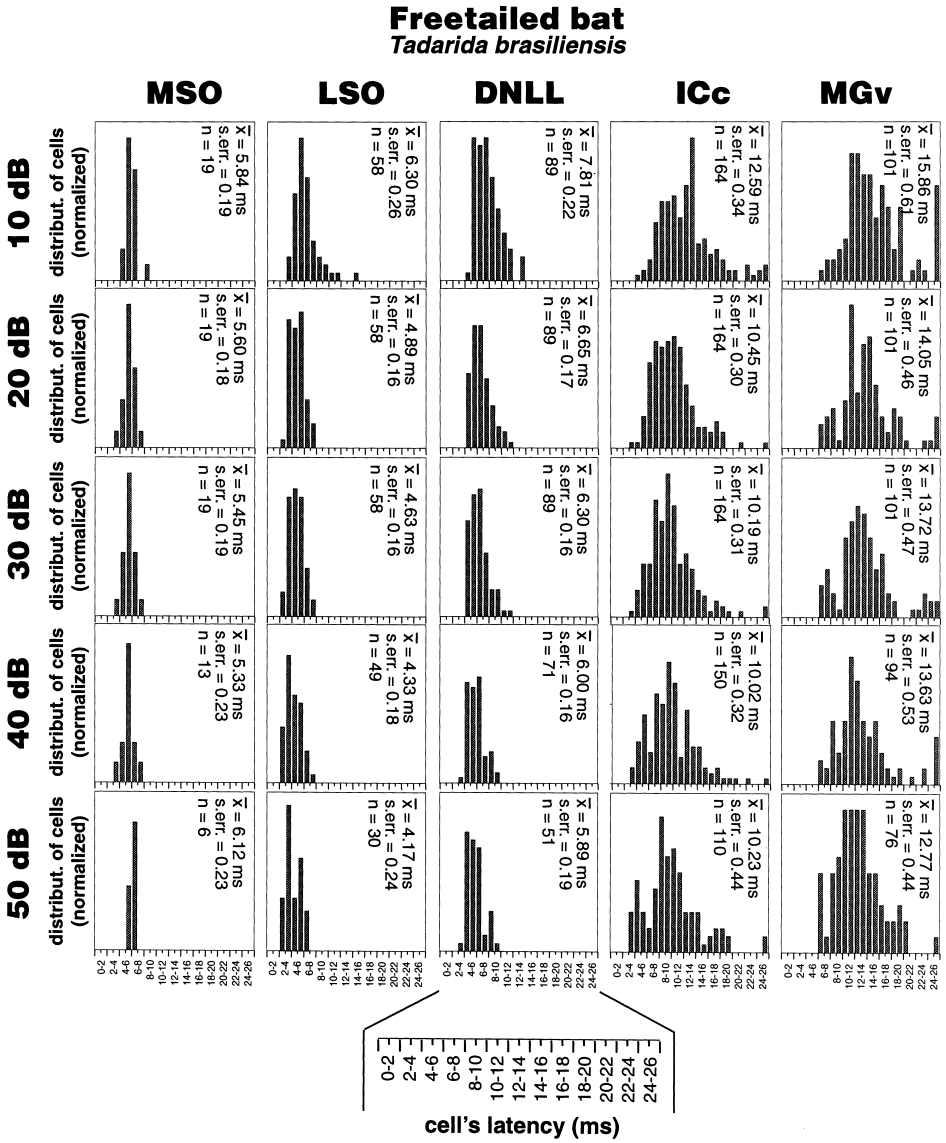

Fig. 2. Distributions of response latency for five nuclei and five intensities. Latency refers to median first spike latency, as shown in Fig. 1, and intensity refers to intensity above threshold for each cell. Stimuli were tones presented at the frequency to which each cell was most sensitive. Distributions are normalized within each graph. ($\bar{x}$ = mean latency; s.err. = standard error; n = number of cells represented in each graph). Bars in histograms and minor tick marks on abscissa represent 1 ms intervals, numbers on abscissa represent 2 ms intervals (for space reasons).

individual cells, and how those features contributed to differences among nuclei. Finally, we will show how central processing, in the form of inhibitory inputs, contributed to those differences.

3.1. Response latencies differed among auditory nuclei

Response latencies and the ranges of latencies we observed varied widely among auditory nuclei. Fig. 2 presents data for each of the five nuclei that we studied in the free-tailed bat. Each nucleus is represented by five histograms, each of which corresponds to a particular sound intensity relative to each cell's threshold. Within a histogram, the bars indicate how many cells had median first spike latencies of a given value. For example, the first histogram (upper left) shows the distribution of first spike latencies for MSO neurons tested with tones presented 10 dB above each cell's threshold. The average first spike latency and standard error for this sample of cells are indicated in the upper right corner of the graph.

There are three main features illustrated in Fig. 2. The first is that average latencies were generally greater at higher synaptic levels regardless of intensity. Average latencies were shortest for the LSO and MSO, and longest for the ICc and MGv. The second main feature is that there was more variability in response latencies between cells at higher synaptic levels. The ICc and the MGv had much wider ranges of latency values compared to the lower nuclei. The third main feature is that there was a general trend for average latencies to shorten with increasing intensity for each of the nuclei (the only deviations from this pattern were that the ICc and MSO showed increases in latency between 40 and 50 dB above threshold).

To facilitate comparisons among the five nuclei, the data described above are re-plotted onto a single graph in Fig. 3. Each curve shows average latency as a function of stimulus intensity above threshold for a particular nucleus. The separation between curves shows the differences in absolute latencies among nuclei, and the slope of each curve shows the general decrease in latency as a function of intensity for each nucleus. It is this latter feature that we will address in detail in the following sections.

While not directly related to the central topic of our study, it is noteworthy that we observed a general increase in latency with decreasing characteristic frequency at each nucleus, of the order of about 1 ms/octave, presumably due to travel time along the cochlear partition (Rhode and Smith, 1986a). A related issue concerns the effects of cochlear travel time on the differences that we observed in absolute latency among nuclei. Since absolute latency increases with decreasing CF, some of the differences in absolute latency that we observed may be due to differences in the CFs of our sample populations. For example, the mean CF of the ICc cells (27.3 kHz) was lower than the mean CF of the LSO cells (32.6 kHz), even though there was considerable overlap in the ranges of CF from these nuclei (Table 1). Based on the difference in CFs, and our estimate of cochlear travel time, we would expect to see longer absolute latencies in the ICc compared to the LSO, but only of the order of about 0.5 ms or less. The observed difference was more of the order of 5.0 ms, indicating that other factors also contributed to the differences in absolute latency that we observed.

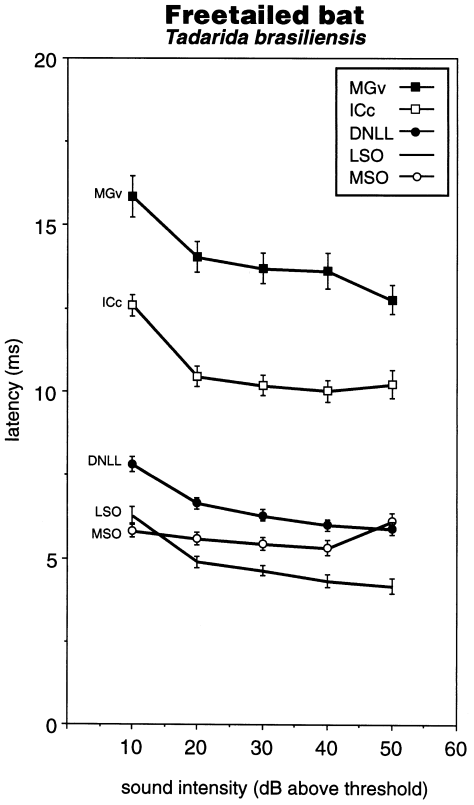

Fig. 3. Summary curves showing average response latency as a function of intensity for five nuclei. Curves were derived from the distribution graphs shown Fig. 2. Error bars indicate the standard error.

Although we noticed the described relationship between (absolute) latency and CF, this report is primarily concerned with (relative) latency *shifts* with intensity. To rule out any effects of CF on latency *shifts*, we analyzed average latency shift as a function of CF for each nucleus. Slopes of linear regression were 0.009 (LSO), −0.002 (DNLL), 0.001 (ICc), −0.0004 (MGv), indicating that CF had no effect on latency changes.

3.2. Intensity-dependent latency change values varied within and between nuclei

The results presented thus far indicate that latencies

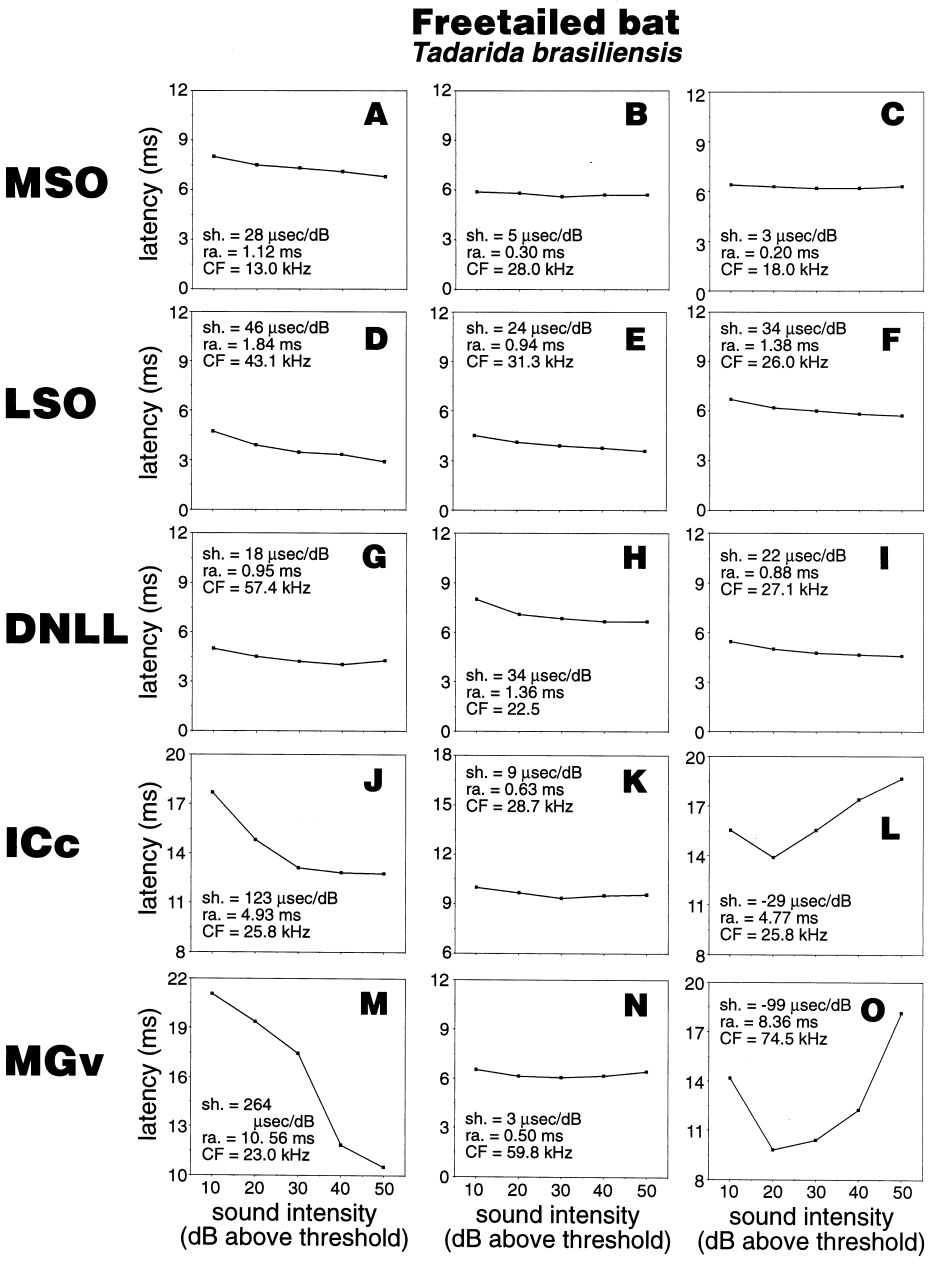

Fig. 4. Latency–intensity functions for three representative cells from each nucleus tested. Measures of latency were derived as described in Fig. 1. Also indicated are average intensity-dependent latency shift values (sh); the range of latencies over which a cell varied (ra); and each cell's CF. Note that the points on each graph represent *median* values. However, to generate a measure of trial-to-trial variability, we calculated the standard error of each point based on the *mean* first spike latency. For every point but one, the standard error was less that 1.2 ms.

within each nucleus generally decreased with increasing stimulus intensities. Our next goal was to examine this feature in more detail by deriving quantitative values of intensity-dependent latency change for each cell in our study.

We began by constructing a latency–intensity function for each cell, and from that function we calculated the average intensity-dependent latency change, as demonstrated in Fig. 1, as well as the range of latencies over which each cell changed. For illustration purposes, Fig. 4 shows the latency–intensity functions of three cells from each nucleus, and the corresponding average latency change with intensity, and range of latency values for these cells. Note that the average latency *change* is calculated from the difference in latency between 10 and 50 dB above the cell's threshold, while the *range* is calculated from the difference between the shortest and the longest latency at any of the tested intensities. For example, the latency range of the cell in Fig. 4O is the latency difference between 20 and 50 dB above

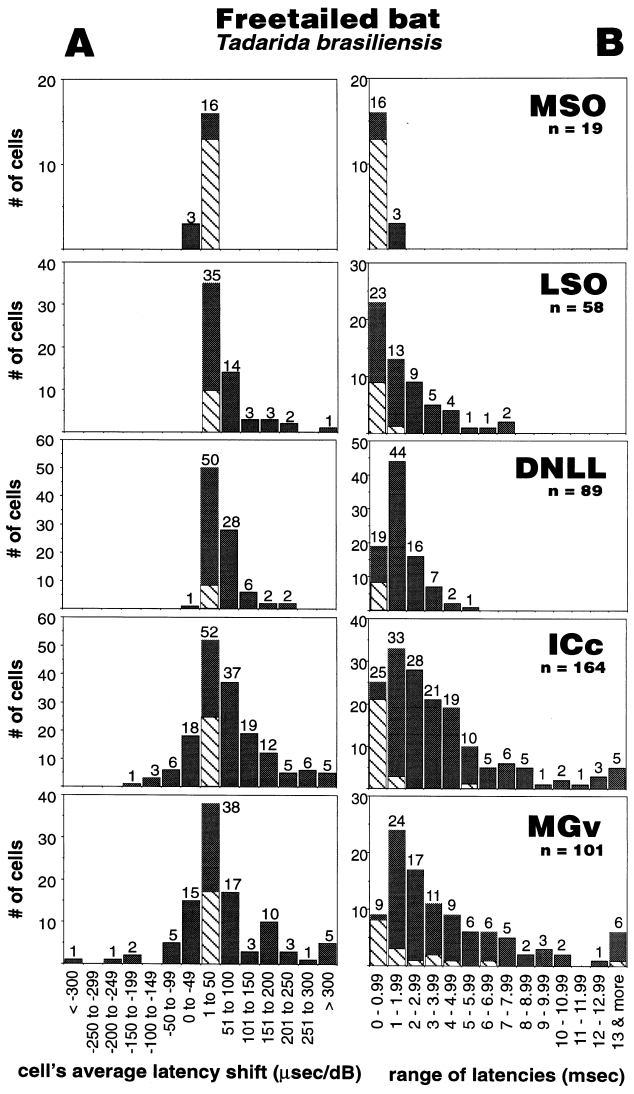

Fig. 5. (A) Distributions of average intensity-dependent latency change values for cells tested in each nucleus. (B) Distributions of ranges of latencies over which cells varied. Hatch marks indicate the positions within the distributions for cells that had small average intensity-dependent latency change values (see text for more detail).

threshold. As Fig. 4 suggests, there was a substantial variability in the quantitative values of latency change and range as well as in the shape of the functions. In the next sections, we will address all three of these issues.

Fig. 5 presents the distributions of average latency change values, and latency ranges for all cells tested in each of the five nuclei. For the distributions in Fig. 5A, each bar indicates the number of cells that had average latency change values within the range indicated below the *x*-axis. Positive values correspond to overall decreases in latency with intensity, while negative values correspond to overall increases in latency with intensity. For example, the peak of each distribution corresponded to an average *decrease* in latency in the range of 1–50 μs/dB.

An obvious feature that emerged from comparing the distributions in Fig. 5A was that values of intensity-dependent latency changes were much more variable at higher synaptic levels. In both the ICc and the MGv, some cells had very large latency change values (e.g. Fig. 4J,M), while other cells had very small latency change values (Fig. 4K,N), and yet other cells had negative latency change values, corresponding to increases in latency with intensity (Fig. 4L,O). In the next section, we will present a more detailed analysis of these divergent patterns of intensity-dependent latency change.

Fig. 5B shows that the range of latencies over which cells varied as a function of intensity also became more variable at higher synaptic levels. This finding seems intuitive, given that Fig. 5A already shows an increase in the variability of average latency change at higher levels. However, an important feature emerges by considering the distributions in Fig. 5A,B together. With the average values alone, we cannot distinguish between cells that have relatively linear changes in latency and cells that may change in nonlinear ways. In other words, one cell might show small, incremental decreases in latency with intensity (corresponding to a narrow range), while another cell might show large increases *and* decreases of similar magnitudes (corresponding to a large range), so that both cells would have similar, small *average* values of latency change. To discriminate between these two possibilities, we identified the cells with small values of average latency change (<20 μs/dB) in both the latency change distributions (Fig. 5A), and in the corresponding range of latency distributions (Fig. 5B). The positions of these cells within the distributions are indicated by hatched marks on the bars. The results show that, for each auditory center, most cells with small values of average latency change also had small ranges over which their latencies changed, indicating that, for these cells at least, average latency change values are not compromised by nonlinearities.

3.3. Patterns of intensity-dependent latency change differed within and between nuclei

To assess how prevalent different patterns of latency change were among the five nuclei, we defined four categories of latency–intensity change (Fig. 6). The first category, 'shallow decreasing latency', encompassed the most prevalent range of intensity-dependent latency changes, 20–200 μs/dB. The second category, 'constant latency', included cells that showed very small average latency changes of less than +20 μs/dB (this category is similar to that defined by Covey and Casseday, 1991).

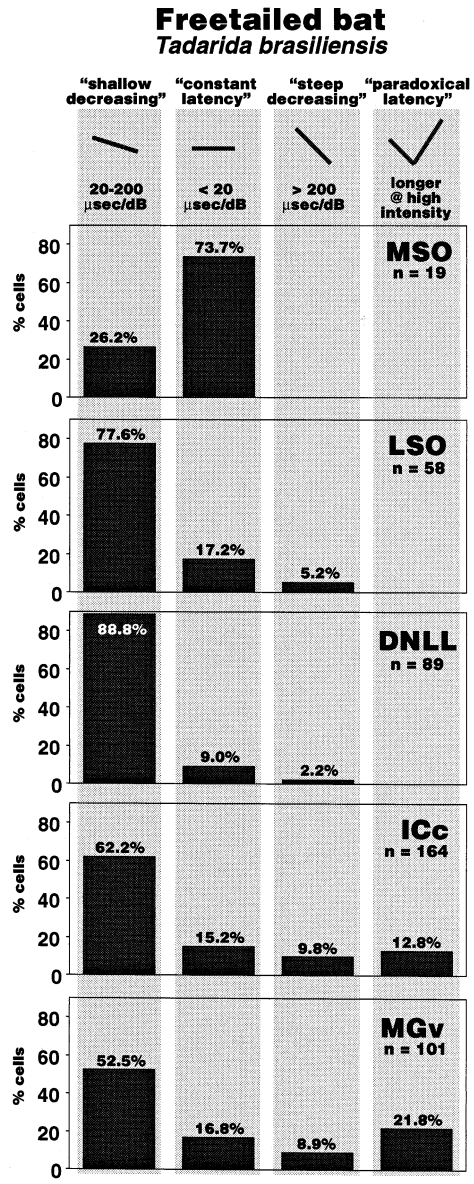

Fig. 6. Distribution of cells for each nucleus according to the pattern of their latency–intensity functions. We defined four patterns: shallow decreasing latency (average latency decrease 20–200 μs/dB); constant latency (average decrease <20 μs/dB); steep decreasing latency (average decrease >200 μs/dB); and paradoxical latency (average latency *increase* >25 μs/dB).

The third category, 'steep decreasing latency', included cells with very large average latency decreases of more than 200 μs/dB. The fourth category, 'paradoxical latency', included cells that had negative average latency changes of at least -25 μs/dB, and thus had longer latencies at higher intensities than at lower intensities (this category is similar to that defined by Sullivan, 1982).

Fig. 6 shows the distributions of cells for each nucleus according to the categories defined above. Several features are apparent. First, cells with paradoxical latency shifts were only observed in the higher nuclei, the ICc and MGv. Second, most of the cells with 'steep decreasing latencies' were also found in the ICc and MGv. Hence, the greater prevalence of cells with these latency patterns – paradoxical latency shift and steep decreasing latency – accounted for the greater range of intensity-dependent latency change values in these nuclei, as shown in Fig. 5. A third notable feature from Fig. 6 is that, while each nucleus had some proportion of constant latency cells, the nucleus with the highest proportion of constant latency cells was the MSO. This finding will be considered further in Section 4.

3.4. GABAergic inhibition shaped paradoxical latency shifts in the ICc

Cells with paradoxical latency shifts were not observed below the ICc (Fig. 6), suggesting that paradoxical latency shifts might be created at the level of the ICc. GABAergic inhibition is known to mediate a variety of transformations that take place at this level (Bauer et al., 2000; Burger and Pollak, 1998; Casseday et al., 1994; Le Beau et al., 1996; Park and Pollak, 1993a; Pollak and Park, 1993; Vater et al., 1992), and for this reason we hypothesized that GABAergic inhibition might also shape paradoxical latency shifts. To test this hypothesis, we iontophoretically applied the $GABA_A$ antagonist bicuculline onto four of the 21 ICc cells with paradoxical latency shifts. In three of these four cells, the paradoxical latency pattern was converted into one of the other latency response patterns (Fig. 7A), suggesting that the paradoxical latency pattern is at least partially created in the inferior colliculus by GABAergic inhibition.

3.5. There was a correspondence between nonmonotonic rate–intensity functions and paradoxical latency–intensity patterns

As mentioned in Section 3.4, inhibition in the ICc has been shown to affect a variety of response properties. In nonmonotonic ICc cells, spike counts increase with intensity, reach a peak, and then decline at higher intensities. For many ICc cells with nonmonotonic rate–intensity functions, the decline in spikes at high intensities is due to inhibition acting at the inferior colliculus (e.g. Pollak and Park, 1993). Since inhibition can shape both nonmonotonic rate–intensity functions and paradoxical latency–intensity functions, we were interested in whether or not there was a correspondence between these two response features. To address this issue, we compared the number of nonmonotonic cells found within each of the four categories of latency patterns in our sample of ICc cells.

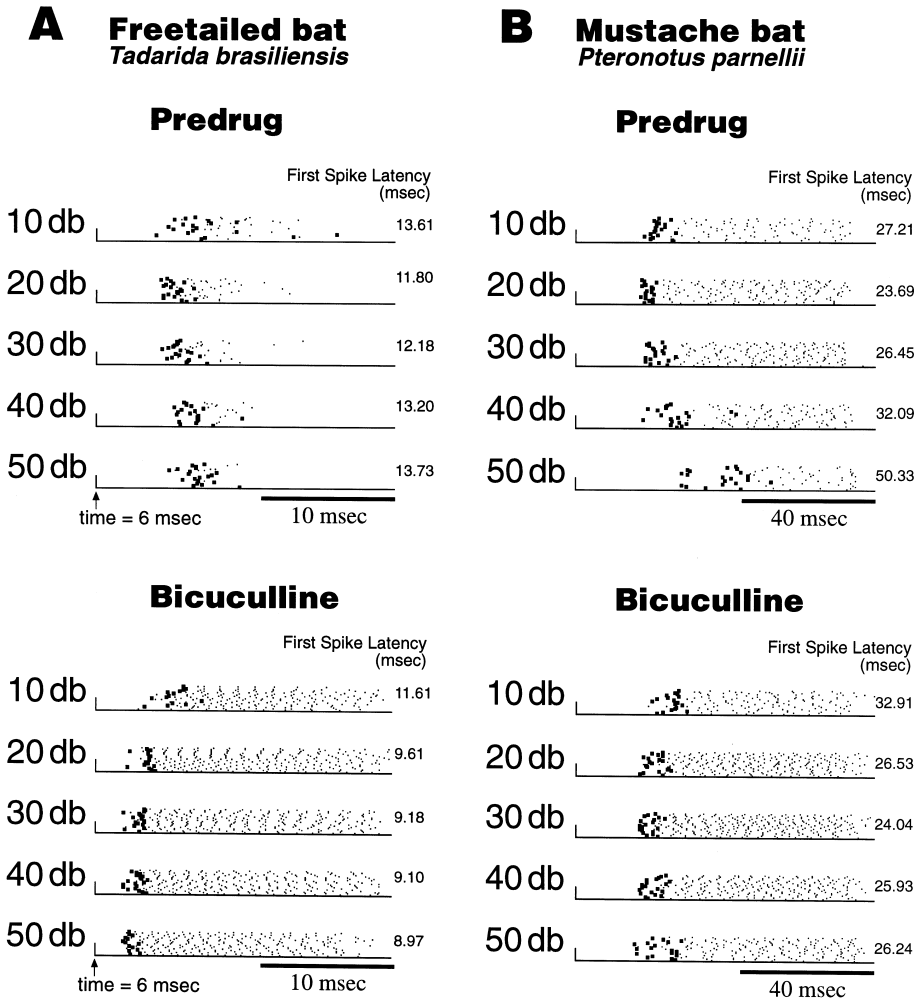

Fig. 7. Effects of applying the GABA antagonist, bicuculline, onto two ICc cells that had paradoxical latency shifts prior to application. (A) Cell was recorded from the free-tailed bat, CF was 27.0 kHz. (B) Cell was recorded from the mustache bat, CF was 60.7 kHz.

We defined a cell's rate–intensity function as nonmonotonic if the spike count first peaked and then decreased by at least 25% at the highest intensity tested. According to this definition, 81 of the 164 (49%) collicular cells in our sample were nonmonotonic. Table 2 shows how these nonmonotonic cells were distributed over the four categories of latency–intensity patterns that we defined previously. Although there was not a strict correspondence between the paradoxical latency shift pattern and the nonmonotonic response pattern, the results support a general trend for paradoxical latency cells to have nonmonotonic rate–intensity functions. About two thirds of the ICc cells with paradoxical latency shifts had nonmonotonic rate–intensity functions. Two thirds of the constant latency cells also had nonmonotonic rate–intensity functions. On the other hand, only about one third of the steep decreasing, and less than half of the shallow decreasing cells had nonmonotonic rate–intensity functions. A χ^2 test, carried out to test the hypothesis of independence between tonicity type and latency pattern, showed that these variables were not independent ($\chi^2 = 9.212$ (df = 3) $P = 0.027$).

Table 2
Correlation between nonmonotonicity and latency–intensity response pattern in the ICc of the free-tailed bat

	All cells	Shallow decreasing latency	Constant latency	Steep decreasing latency	Paradoxical latency
Total number of cells	164	102	25	16	21
Nonmonotonic cells	81 (49%)	45 (44%)	17 (68%)	5 (31%)	14 (67%)
Monotonic cells	83 (51%)	57 (56%)	8 (32%)	11 (69%)	7 (33%)

3.6. Thresholds were not a significant factor in shaping latency patterns

Excitatory thresholds are an important factor in determining constant latency patterns in the columnar area of the ventral nucleus of the lateral lemniscus (VNLLc), a brainstem region that is dominated by constant latency neurons (Covey and Casseday, 1991). To determine if thresholds might also play a part in shaping the constant latency functions that we observed in the present study, we compared thresholds among the four latency patterns that we defined, and found that the constant latency cells had only slightly higher thresholds compared to cells with the other pattern types. The average threshold for the constant latency cells was 10.4 dB SPL. Average thresholds for the shallow decreasing, steep decreasing, and paradoxical cells were 7.5 dB, 6.3 dB, and 5.7 dB, respectively. An analysis of variance indicated that thresholds did not differ significantly among the four pattern types ($F = 1.173$ (df = 3,160) $P = 0.32$), nor did thresholds differ between the constant latency cells compared to the thresholds of the pooled, nonconstant latency cells ($F = 2.794$ (df = 1,162) $P = 0.10$).

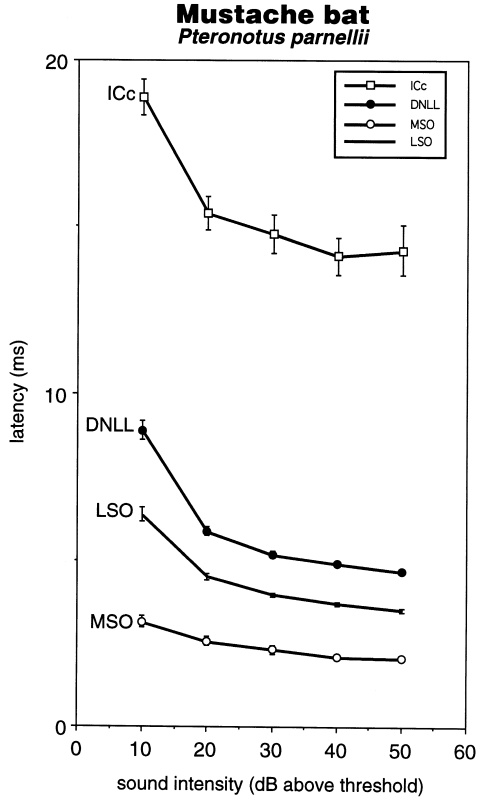

Fig. 8. Mustache bat summary curves showing average absolute response latency as a function of intensity for four nuclei. Figure compares to Fig. 3. Error bars indicate the standard error.

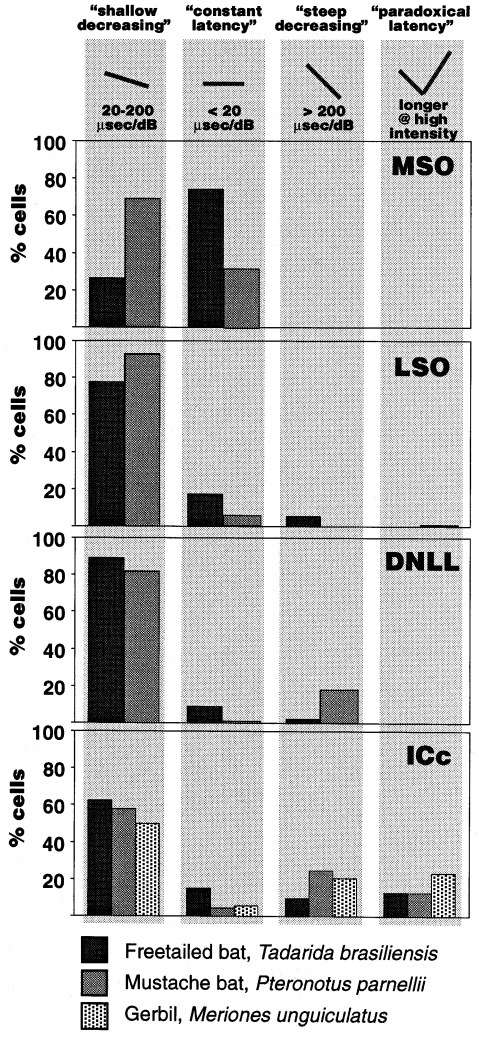

Fig. 9. Distribution of cells from the free-tailed bat, mustache bat, and gerbil according to the pattern of their latency–intensity functions: shallow decreasing latency; constant latency; steep decreasing latency; and paradoxical latency. Figure compares to Fig. 6.

3.7. Results from the mustache bat were consistent with those from the free-tailed bat

To determine if the results described in the previous sections are species-specific or general, we repeated the types of analyses presented in the previous sections with data from two other species. Specifically, we analyzed latency data from the LSO, MSO, DNLL, and ICc of the mustache bat (*Pteronotus parnellii*) and from the ICc of the Mongolian gerbil (*Meriones unguiculatus*). The results indicate that many of the features described above for the free-tailed bat were similar across the other species tested. In the following paragraphs we will present a brief summary of our comparative findings.

Fig. 8 shows mean absolute latency as a function of intensity for nuclei in the mustache bat, presented in the

same format as used in Fig. 3 to describe the free-tailed bat data. While there were some differences between the two species, the general characteristics of the curves were comparable. For both species, there was a tendency for cells at progressively higher synaptic levels to have longer absolute response latencies, and there was a tendency for populations of cells in both species to show a decrease in latency with increasing intensity.

Individual cells from the mustache bat and the gerbil displayed the same variety of latency–intensity patterns as seen in the free-tailed bat. Fig. 9 shows the distribution of cells from the mustache bat and the gerbil across latency–intensity patterns for each nucleus. For ease of comparison, this figure also includes the free-tailed bat data from Fig. 6. One of the key features illustrated in Fig. 9 is that, for both bat species, cells with the paradoxical latency change pattern were not observed below the ICc, and for all three species, paradoxical latency cells were observed in the ICc. Fig. 9 also shows that the two bat species differed with regard to the distribution of latency patterns in the MSO, a topic that will be addressed in Section 4.

Because we have examined only one nucleus in the gerbil auditory system, the gerbil data do not directly address the question of changes in latency functions across nuclei. However, for the one center studied, the ICc, the distribution of latency pattern types for the gerbil is remarkably similar to those obtained from the two bat species (Fig. 9), suggesting that the different latency patterns we observed are a general feature, not specific to bats.

To verify pharmacologically that paradoxical latency shifts are also formed de novo in the mustache bat ICc, we tested four paradoxical latency cells with the iontophoretic application of the GABA antagonist bicuculline (the same procedure as followed for the free-tailed bat). In three of these four cells, the paradoxical latency pattern was converted into one of the three other response patterns (Fig. 7B), suggesting that GABAergic inhibition participates in shaping this property in the mustache bat ICc.

4. Discussion

Our study shows that central processing contributes to intensity-dependent latency changes in the auditory system. The four main findings of our study are: (1) the range of intensity-dependent latency change values increases considerably at higher synaptic levels; (2) paradoxical latency shifts are observed only at the higher synaptic levels that we tested; (3) inhibition shapes intensity-dependent latency change in the inferior colliculus; and (4) these results are similar across the species we tested.

4.1. Comparison with other studies

We are not aware of any studies from bats that have examined intensity-dependent latency change in the auditory nerve. However, there are data from the cat. The latencies of *cat* auditory nerve fibers (Antoli-Candela and Kiang, 1978; Heil and Irvine, 1997) and cells in the anteroventral cochlear nucleus (AVCN) (Kitzes et al., 1978), which receive their principal inputs from auditory nerve fibers, shorten considerably with increasing intensity within the first 10 dB of threshold. For higher intensities, their latencies continue to shorten, but in a much less dramatic fashion. Hence, when we apply our classification scheme to latency–intensity functions from auditory nerve fibers and AVCN cells (excluding latencies for intensities below 10 dB above threshold to be consistent with our data), we would classify those functions as 'shallow decreasing'. This observation supports the notion that, at higher levels of the auditory system, deviations from the shallow decreasing pattern are the result of neural processing. However, while intensity-dependent latency changes have been widely observed throughout the auditory system from cochlea to cortex, prior to the present study, there has been little effort to quantify this effect on a population level, either within a particular nucleus or among nuclei. The reason for this lack of information may be that intensity-dependent latency change traditionally has been viewed as a byproduct of signal transduction (Eccles, 1964), an effect that the nervous system has to deal with, but not something that the nervous system might actively incorporate, or modify, in processing information. There are, however, several recent lines of investigation that have focused on specific aspects of intensity-dependent latency change, aside from simply documenting the phenomenon. Those investigations have focused on: (1) stimulus parameters that affect first spike latency; (2) neurons that exhibit very little latency change with intensity (constant latency neurons); (3) neurons that display paradoxical latency shifts; and (4) neurons that are sensitive to interaural intensity differences, and show effects of intensity-dependent latency change on their interaural intensity difference (IID) sensitivity. Each of these topics will be considered below.

4.2. Stimulus parameters that affect first spike latency

First spike latency is commonly associated with the transient onset portion of a stimulus (Heil, 1997a), which, in turn, is affected by a number of physical stimulus parameters. In a recent series of experiments, Heil and Irvine (Heil, 1997a,b; Heil and Irvine, 1996, 1997) explored how response latency is affected by the duration of the rise time, the rate of change in sound pres-

sure during the rise time, and the acceleration of peak pressure during the rise time (the change in rate of change). They found that holding the rise time constant and varying the rate of change in sound pressure (as we did in our study by varying the intensity of the steady-state portion of the stimuli at the end of the rise time) generated different first spike latencies. However, they also found that holding the rate of change in sound pressure constant and varying the rise time also generated different first spike latencies, indicating that latency as a function of change in sound pressure was not independent of rise time. A much better fit for the data was obtained when latency was re-plotted as a function of acceleration of pressure. In this case, first spike latency was an invariant function of the maximum acceleration of pressure, independent of rise time or rate of change in sound pressure, per se.

An important conclusion from Heil and Irvine's work is that researchers studying first spike latency should be careful in interpreting data based on stimuli that vary in steady-state intensity, but have a constant rise time, because this commonly used procedure causes co-variations in acceleration of pressure, the stimulus feature that appears to be more important in determining first spike latency. In our present report, none of the studies cited, except those of Heil and Irvine, evaluated acceleration of pressure, and, because different studies used different rise times, comparisons of data across studies are difficult to interpret.

In our own experiments, we did not vary rise time, and we did not evaluate the effects of acceleration of pressure during the rise time. However, because we used a very short rise time of 0.2 ms, accelerations of peak pressure were always very high at each intensity used. Heil and Irvine used much longer rise times (between 1.7 and 85 ms), which produced much lower accelerations. They observed the greatest changes in latency for relatively low maximum accelerations (between 1.0×10^{-1} and 1.0×10^{3} $\mu Pa/s^2$). In comparison, the maximum accelerations produced by the tone bursts used in this study were always high (between 2.4×10^{3} and 7.8×10^{6} $\mu Pa/s^2$) and thus should have produced much smaller changes in latency than those observed by Heil and Irvine.

More importantly, as we used the same stimuli to compare latency functions from cells in different auditory centers, any co-variation of acceleration with steady-state intensity should have been the same for each brain region tested. Hence, while we cannot distinguish to what degree the latency changes that we observed for individual cells were due to changes in peak steady-state intensity versus changes in maximum acceleration of pressure during the rise time, we feel confident that the transformations we observed in latency change from nucleus to nucleus are valid.

4.3. Constant latency neurons

Constant latency neurons and neurons with paradoxical latency change have been associated with temporal processing. Constant latency neurons have been suggested to play a role in precisely marking the arrival time of a stimulus, independent of absolute intensity (Covey and Casseday, 1991). Constant latency neurons have been found in the ICc (Bodenhamer and Pollak, 1981; Suga, 1970), the DNLL (Covey, 1993), and in the intermediate and ventral (VNLL) nuclei of the lateral lemniscus (Covey and Casseday, 1991; Batra and Fitzpatrick, 1999). Within the VNLL of the big brown bat (*Eptesicus fuscus*), the columnar area (VNLLc) appears to be specialized in that it is dominated by constant latency neurons (Covey and Casseday, 1991).

Consistent with these previous findings, we found constant latency neurons in all nuclei tested. Hence, it appears that constant latency neurons are common to many nuclei and synaptic levels. One interesting observation was that the proportion of constant latency cells was substantially higher in the free-tailed bat MSO compared to the mustache bat MSO. The reason for this finding is unclear, but the differential patterns of innervation to the free-tailed bat MSO and the mustache bat MSO may account for this difference (Grothe et al., 1992, 1994; Covey et al., 1991; Grothe, 1994).

For constant latency cells in the VNLLc, Covey and Casseday (1991) suggested that excitatory thresholds were an important factor in determining the constant latency pattern. However, in our data from the ICc, we did not find significantly higher thresholds for constant latency cells compared to cells with other latency patterns, suggesting that different mechanisms may shape the constant latency pattern in different nuclei.

4.4. Neurons with paradoxical latency change

Neurons with paradoxical latency change are also associated with temporal processing, presumably playing a role in coding time intervals between successive stimuli of different intensities. Paradoxical latency cells have been suggested to function in processing complex communication signals (Margoliash, 1983; Hall and Feng, 1986; Olsen and Suga, 1991b; Suga, 1988). In bats, these cells are believed to be associated with processing target range information from paired call-echo stimuli (e.g. Sullivan, 1982; Berkowitz and Suga, 1989; Olsen and Suga, 1991b; Suga, 1988). Neurons sensitive to target range respond best to a particular delay between a loud, emitted call and a soft, returning echo. Sensitivity is achieved by the coincidence of a long latency response evoked by the loud call and a short latency response evoked by the soft, returning echo.

Hence, their sensitivity is directly related to the different response latencies generated by the different intensities of call and echo.

Previous reports have indicated that paradoxical latency cells are much more common in the inferior colliculus and above (Berkowitz and Suga, 1989; Olsen and Suga, 1991a,b; Rose et al., 1963; Suga, 1970; Sullivan, 1982) than in the nuclei below the inferior colliculus. Suga and his colleagues have proposed that inhibition plays a key role in shaping paradoxical latency shifts (Berkowitz and Suga, 1989; Olsen and Suga, 1991b). Our finding that six of eight paradoxical ICc cells changed their latency patterns with local application of bicuculline (Fig. 7) is consistent with all of these previous findings and suggests that paradoxical latency change is to some degree a response property created at the ICc. It is notable, however, that paradoxical cells have been reported in two brain stem regions, namely the nuclei of the lateral lemniscus (Aitkin et al., 1970; Covey, 1993), and the dorsal cochlear nucleus (Rose et al., 1959; Rhode and Smith, 1986b).

Not only were the ICc and the MGv the only nuclei in our study that had cells with paradoxical latency changes, they were also the nuclei with the highest proportions of cells that had steep decreasing latency functions. Hence, the ICc and MGv cell populations had the greatest ranges of intensity-dependent latency change values from steep decreasing to increasing (Figs. 5 and 6). As discussed below, a wide range of intensity-dependent latency change values has important implications for the processing of interaural intensity differences.

4.5. *Effects of intensity-dependent latency change on interaural intensity difference sensitivity*

IIDs are important cues for localizing sounds in space. Neurons that are sensitive to IIDs are primarily excited by stimulation of one ear and primarily inhibited by stimulation of the other ear (e.g. Erulkar, 1972; Goldberg and Brown, 1969). Thus, the response characteristics of an IID-sensitive cell reflect an integration of excitatory and inhibitory actions such that, in general, a sound that is more intense at the ear providing excitation evokes spikes, while a sound that is more intense at the ear providing inhibition suppresses spikes. However, there is much variability among cells as to what range of IIDs evoke maximum, intermediate, and minimum spike counts. In other words, different cells are sensitive to different ranges of IIDs, a feature that makes it possible for populations of cells to encode the entire range of IIDs that an animal would encounter in nature (Irvine and Gago, 1990; Park, 1998; Park et al., 1996, 1997; Sanes and Rubel, 1988).

The IID sensitivity of an individual cell is determined by a number of factors related to its excitatory/inhibitory pattern of innervation. One factor is the degree of coincidence between the excitation and inhibition, a factor that is particularly relevant to our present study since coincidence can be significantly affected by intensity-dependent latency change (Jeffress, 1948; Irvine et al., 1995; Yin et al., 1985; Pollak, 1988; Park, 1998; Park et al., 1996) or, as Heil (1998) pointed out, by interaural transient envelope disparities. As an example, consider a cell with shallow decreasing latency–intensity functions for both excitation and inhibition. The latencies of both inputs will vary with IID, and they will vary in opposite directions. The excitation will tend to have its shortest latencies for IIDs that involve greater intensity at the ear providing excitation, while the inhibition will tend to have its shortest latencies for IIDs that involve greater intensity at the ear providing inhibition. Since the latencies of both excitation and inhibition vary with IID, the degree of coincidence will also vary with IID, making intensity-dependent latency change a significant aspect of IID sensitivity.

In the present study, we found that different nuclei had different ranges of latency change with intensity (Fig. 5). This observation suggests that intensity-dependent latency change might affect IID sensitivity differently for different nuclei, and this effect might account for some of the differences in IID sensitivity recently reported for the LSO and ICc (Irvine and Gago, 1990; Park, 1998; Park et al., 1997; Sanes and Rubel, 1988).

5. Conclusion

Intensity-dependent latency change could be viewed as being particularly problematic for the auditory system because many aspects of auditory processing depend heavily on precise timing. However, an intriguing possibility is that the auditory system may use and modify intensity-dependent latency changes in different ways, enabling different cells to participate in different functions, such as encoding IIDs, arrival time information, or complex, multi-component signals. Hence, intensity-dependent latency change may be a valuable tool for auditory information processing.

Acknowledgements

We give our special thanks to George D. Pollak for his kindness, generosity, and expertise in mentoring and inspiring each of us. We thank C. Resler for technical support, and two anonymous reviewers for their thoughtful suggestions. This work was supported by NIH Grant DC02850 (T.J.P.), NIH Grant DC20068

(G.D. Pollak), SFB 204 (B.G.), and the Alexander-von-Humboldt Foundation (T.J.P.).

References

Aitkin, L.M., Dunlop, C.W., 1968. Interplay of excitation and inhibition in the cat medial geniculate body. J. Neurophysiol. 31, 44–61.

Aitkin, L.M., Anderson, D.J., Brugge, J.F., 1970. Tonotopic organization and discharge characteristics of single neurons in nuclei of the lateral lemniscus of the cat. J. Neurophysiol. 33, 421–440.

Antoli-Candela, J.F., Kiang, N.Y.S., 1978. Unit activity underlying the N1 potential. In: Naunton, R.F., Fernandez, C. (Eds.), Evoked Activity in the Auditory Nervous System. Academic Press, New York, pp. 165–191.

Batra, R., Fitzpatrick, D.C., 1999. Discharge patterns of neurons in the ventral nucleus of the lateral lemniscus of the unanesthetized rabbit. J. Neurophysiol. 82, 1097–1113.

Bauer, E.E., Klug, A., Pollak, G.D., 2000. Features of contralaterally evoked inhibition in the inferior colliculus. Hear. Res. 141, 80–96.

Berkowitz, A., Suga, N., 1989. Neural mechanisms of ranging are different in two species of bats. Hear. Res. 41, 255–264.

Bodenhamer, R.D., Pollak, G.D., 1981. Time and frequency domain processing in the inferior colliculus of echolocating bats. Hear. Res. 5, 317–335.

Brugge, J.F., Dubrovsky, N.A., Aitkin, L.M., Anderson, D.J., 1969. Sensitivity of single neurons in auditory cortex of cat to binaural tonal stimulation; effects of varying interaural time and intensity. J. Neurophysiol. 32, 1005–1024.

Burger, R.M., Pollak, G.D., 1998. Analysis of the role of inhibition in shaping responses to sinusoidally amplitude-modulated signals in the inferior colliculus. J. Neurophysiol. 80, 1686–1701.

Carney, T., Paradiso, M.A., Freeman, R.D., 1989. A physiological correlate of the Pulfrich effect in cortical neurons of the cat. Vision Res. 29, 155–165.

Casseday, J.H., Ehrlich, D., Covey, E., 1994. Neural tuning for sound duration: role of inhibitory mechanisms in the inferior colliculus. Science 264, 847–850.

Covey, E., 1993. Response properties of single units in the dorsal nucleus of the lateral lemniscus and paralemniscal zone of an echolocating bat. J. Neurophysiol. 69, 842–859.

Covey, E., Casseday, J.H., 1991. The monaural nuclei of the lateral lemniscus in an echolocating bat: parallel pathways for analyzing temporal features of sound. J. Neurosci. 11, 3456–3470.

Covey, E., Casseday, J.H., 1999. Timing in the auditory system of the bat. Annu. Rev. Physiol. 61, 457–476.

Covey, E., Vater, M., Casseday, J.H., 1991. Binaural properties of single units in the superior olivary complex of the mustached bat. J. Neurophysiol. 66, 1080–1094.

Deatherage, B.H., Eldredge, D.H., Davis, H., 1959. Latency of action potentials in the cochlea of the guinea pig. J. Acoust. Soc. Am. 31, 479–486.

Eccles, J.C., 1964. The Physiology of Synapses. Springer, Berlin.

Erulkar, S.D., 1972. Comparative aspects of spatial localization of sound. Physiol. Rev. 52, 237–360.

Goldberg, J.M., Brown, P.B., 1969. Response of binaural neurons of dog superior olivary complex to dichotic tonal stimuli: some physiological mechanisms of sound localization. J. Neurophysiol. 32, 613–636.

Goldberg, J.M., Brownell, W.E., 1973. Discharge characteristics of neurons in anteroventral and dorsal cochlear nuclei of cat. Brain Res. 64, 35–54.

Grothe, B., 1994. Interaction of excitation and inhibition in processing of pure tone and amplitude-modulated stimuli in the medial superior olive of the mustached bat. J. Neurophysiol. 71, 706–721.

Grothe, B., Park, T.J., 1998. Sensitivity to interaural time differences in the medial superior olive of a small mammal, the Mexican free-tailed bat. J. Neurosci. 18, 6608–6622.

Grothe, B., Vater, M., Casseday, J.H., Covey, E., 1992. Monaural interaction of excitation and inhibition in the medial superior olive of the mustached bat: an adaptation for biosonar. Proc. Natl. Acad. Sci. USA 89, 5108–5112.

Grothe, B., Schweizer, H., Pollak, G.D., Schuller, G., Rosemann, C., 1994. Anatomy and projection patterns of the superior olivary complex in the Mexican free-tailed bat, *Tadarida brasiliensis mexicana*. J. Comp. Neurol. 343, 630–646.

Hall, J., Feng, A.S., 1986. Neural analysis of temporally patterned sounds in the frog's thalamus: processing of pulse duration and pulse repetition rate. Neurosci. Lett. 63, 215–220.

Haplea, S., Covey, E., Casseday, J.H., 1994. Frequency tuning and response latencies at three levels in the brainstem of the echolocating bat, *Eptesicus fuscus*. J. Comp. Physiol. A 174, 671–683.

Havey, D.C., Caspary, D.M., 1980. A simple technique for constructing 'piggy-back' multibarrel microelectrodes. Electroencephalogr. Clin. Neurophysiol. 48, 249–251.

Heil, P., 1997a. Auditory cortical onset responses revisited. I. First-spike timing. J. Neurophysiol. 77, 2616–2641.

Heil, P., 1997b. Auditory cortical onset responses revisited. II. Response strength. J. Neurophysiol. 77, 2642–2660.

Heil, P., 1998. Further observations on the threshold model of latency for auditory neurons [comment]. Behav. Brain Res. 95, 233–236.

Heil, P., Irvine, D.R., 1996. On determinants of first-spike latency in auditory cortex. NeuroReport 7, 3073–3076.

Heil, P., Irvine, D.R., 1997. First-spike timing of auditory-nerve fibers and comparison with auditory cortex. J. Neurophysiol. 78, 2438–2454.

Heil, P., Irvine, D.R., 1998. The posterior field P of cat auditory cortex: coding of envelope transients. Cereb. Cortex 8, 125–141.

Hind, J.E., Goldberg, J.M., Greenwood, D.D., Rose, J.E., 1963. Some discharge characteristics of single neurons in the inferior colliculus of the cat. II. Timing of the discharges and observations on binaural stimulation. J. Neurophysiol. 26, 321–341.

Irvine, D.R., Gago, G., 1990. Binaural interaction in high-frequency neurons in inferior colliculus of the cat: effects of variations in sound pressure level on sensitivity to interaural intensity differences. J. Neurophysiol. 63, 570–591.

Irvine, D.R., Park, V.N., Mattingley, J.B., 1995. Responses of neurons in the inferior colliculus of the rat to interaural time and intensity differences in transient stimuli: Implications for the latency hypotheses. Hear. Res. 85, 127–141.

Jeffress, L.A., 1948. A place theory of sound localisation. J. Comp. Psychol. 41, 35–39.

Kitzes, L.M., Gibson, M.M., Rose, J.E., Hind, J.E., 1978. Initial discharge latency and threshold considerations for some neurons in cochlear nuclear complex of the cat. J. Neurophysiol. 41, 1165–1182.

Klug, A., Bauer, E.E., Pollak, G.D., 1999. Multiple components of ipsilaterally evoked inhibition in the inferior colliculus. J. Neurophysiol. 82, 593–610.

Kolehmainen, K., Keskinen, E., 1974. Evidence for the latency-time explanation of the Pulfrich phenomenon. Scand. J. Psychol. 15, 320–321.

Le Beau, F.E., Rees, A., Malmierca, M.S., 1996. Contribution of GABA- and glycine-mediated inhibition to the monaural temporal response properties of neurons in the inferior colliculus. J. Neurophysiol. 75, 902–919.

Lit, A., 1949. The magnitude of the Pulfrich stereophenomenon as a function of binocular differences of intensity at various levels of illumination. Am. J. Psychol. 62, 159–181.

Margoliash, D., 1983. Acoustic parameters underlying the responses of song-specific neurons in the white-crowned sparrow. J. Neurosci. 3, 1039–1057.

Møller, A.R., 1975. Latency of unit responses in cochlear nucleus determined in two different ways. J. Neurophysiol. 38, 812–821.

Mountcastle, V.B., Davies, P.W., Berman, A.L., 1957. Response properties of neurons of cat's somatic sensory cortex to peripheral stimuli. J. Neurophysiol. 20, 374–407.

Oertel, D., 1999. The role of timing in the brain stem auditory nuclei of vertebrates. Annu. Rev. Physiol. 61, 497–519.

Olsen, J.F., Suga, N., 1991a. Combination-sensitive neurons in the medial geniculate body of the mustached bat: encoding of relative velocity information. J. Neurophysiol. 65, 1254–1274.

Olsen, J.F., Suga, N., 1991b. Combination-sensitive neurons in the medial geniculate body of the mustached bat: encoding of target range information. J. Neurophysiol. 65, 1275–1296.

Oswald, J.P., Klug, A., Park, T.J., 1999. Interaural intensity difference processing in auditory midbrain neurons: Effects of a transient early inhibitory input. J. Neurosci. 19, 1149–1163.

Park, T.J., 1998. IID sensitivity differs between two principal centers in the interaural intensity difference pathway: the LSO and the IC. J. Neurophysiol. 79, 2416–2431.

Park, T.J., Pollak, G.D., 1993a. GABA shapes a topographic organization of response latency in the mustache bat's inferior colliculus. J. Neurosci. 13, 5172–5187.

Park, T.J., Pollak, G.D., 1993b. GABA shapes sensitivity to interaural intensity disparities in the mustache bat's inferior colliculus: implications for encoding sound location. J. Neurosci. 13, 2050–2067.

Park, T.J., Grothe, B., Pollak, G.D., Schuller, G., Koch, U., 1996. Neural delays shape selectivity to interaural intensity differences in the lateral superior olive. J. Neurosci. 16, 6554–6566.

Park, T.J., Monsivais, P., Pollak, G.D., 1997. Processing of interaural intensity differences in the LSO: Role of interaural threshold differences. J. Neurophysiol. 77, 2863–2878.

Pollak, G.D., 1988. Time is traded for intensity in the bat's auditory system. Hear. Res. 36, 107–124.

Pollak, G.D., Park, T.J., 1993. The effects of GABAergic inhibition on monaural response properties of neurons in the mustache bat's inferior colliculus. Hear. Res. 65, 99–117.

Pulfrich, C., 1922. Die Stereoskopie im Dienste der isochromen und heterochromen Photometrie. Naturwissenschaften 10, 553–564, 569–574, 596–601, 714–722, 735–743, 751–761.

Rhode, W.S., Smith, P.H., 1986a. Encoding timing and intensity in the ventral cochlear nucleus of the cat. J. Neurophysiol. 56, 261–268.

Rhode, W.S., Smith, P.H., 1986b. Physiological studies on neurons in the dorsal cochlear nucleus of the cat. J. Neurophysiol. 56, 287–307.

Rose, J.E., Galambos, R., Hughes, J.R., 1959. Microelectrode studies of the cochlear nuclei of the cat. Bull. Johns Hopkins Hosp. 104, 211–251.

Rose, J.E., Greenwood, D.D., Goldberg, J.M., Hind, J.E., 1963. Some discharge characteristics of single neurons in the inferior colliculus of the cat. I. Tonotopical organization, relation of spike-counts to tone intensity, and firing patterns of single elements. J. Neurophysiol. 26, 294–320.

Sanes, D.H., Rubel, E.W., 1988. The ontogeny of inhibition and excitation in the gerbil lateral superior olive. J. Neurosci. 8, 682–700.

Schuller, G., Radtke-Schuller, S., Betz, M., 1986. A stereotaxic method for small animals using experimentally determined reference profiles. J. Neurosci. Methods 18, 339–350.

Suga, N., 1970. Echo-ranging neurons in the inferior colliculus of bats. Science 170, 449–452.

Suga, N., 1988. Auditory neuroethology and speech processing: complex-sound processing by combination-sensitive neurons. In: Edelman, G.M., Gall, W.E.N., C.W. (Eds.), Auditory Function. John Wiley and Sons, New York, pp. 679–720.

Sullivan, W.E., 1982. Possible neural mechanisms of target distance coding in auditory system of the echolocating bat *Myotis lucifugus*. J. Neurophysiol. 48, 1033–1047.

Vater, M., Habbicht, H., Kossl, M., Grothe, B., 1992. The functional role of GABA and glycine in monaural and binaural processing in the inferior colliculus of horseshoe bats. J. Comp. Physiol. A 171, 541–553.

Yang, L., Pollak, G.D., 1994a. Binaural inhibition in the dorsal nucleus of the lateral lemniscus of the mustache bat affects responses for multiple sounds. Audit. Neurosci. 1, 1–17.

Yang, L., Pollak, G.D., 1994b. The roles of GABAergic and glycinergic inhibition on binaural processing in the dorsal nucleus of the lateral lemniscus of the mustache bat. J. Neurophysiol. 71, 1999–2013.

Yin, T.C., Hirsch, J.A., Chan, J.C., 1985. Responses of neurons in the cat's superior colliculus to acoustic stimuli. II. A model of interaural intensity sensitivity. J. Neurophysiol. 53, 746–758.